



**HAL**  
open science

## Hydrogenation reactions and adsorption: From CO to methanol on a graphene surface

Sabine Morisset, Nathalie Rougeau, Dominique Teillet-Billy

► **To cite this version:**

Sabine Morisset, Nathalie Rougeau, Dominique Teillet-Billy. Hydrogenation reactions and adsorption: From CO to methanol on a graphene surface. *Molecular Astrophysics*, 2019, 14, pp.1-9. 10.1016/j.molap.2019.02.001 . hal-02063452

**HAL Id: hal-02063452**

**<https://hal.science/hal-02063452>**

Submitted on 22 Oct 2021

**HAL** is a multi-disciplinary open access archive for the deposit and dissemination of scientific research documents, whether they are published or not. The documents may come from teaching and research institutions in France or abroad, or from public or private research centers.

L'archive ouverte pluridisciplinaire **HAL**, est destinée au dépôt et à la diffusion de documents scientifiques de niveau recherche, publiés ou non, émanant des établissements d'enseignement et de recherche français ou étrangers, des laboratoires publics ou privés.



Distributed under a Creative Commons Attribution - NonCommercial 4.0 International License

# Hydrogenation reactions and adsorption : from CO to methanol on a graphene surface

Sabine Morisset<sup>1</sup>, Nathalie Rougeau, Dominique Teillet-Billy

*Institut des Sciences Molculaires d'Orsay, ISMO, CNRS, Université Paris-Sud, Université Paris Saclay, F-91405 Orsay, France*

---

## Abstract

Successive hydrogenation reactions of isolated CO molecules adsorbed on a bare graphene surface have been studied by density functional theory using a van der Waals functional. Three hydrogenation scenarios, leading to the formation of methanol via the intermediate species: HCO, H<sub>2</sub>CO, HCOH, H<sub>3</sub>CO and H<sub>2</sub>COH, have been considered. Hydrogenation and adsorption energies on the surface have been calculated for all the species. The fractions of molecules released in the gas phase after formation on the surface have been calculated with two different chemical desorption models. Our results show that the fraction of methanol molecules released in the gas phase is low (< 6%) whatever the scenario. Conversely, the highest fractions of molecules released in the gas phase have been obtained for formaldehyde, H<sub>2</sub>CO, and the hydroxymethyl radical, H<sub>2</sub>COH. The methoxy radical, H<sub>3</sub>CO, is characterized by a high adsorption energy on the substrate (−0.337eV).

---

## 1. Introduction

In the interstellar medium (ISM), the methanol (CH<sub>3</sub>OH) molecule is detected in interstellar clouds with abundances relative to H<sub>2</sub> of 10<sup>−6</sup>-10<sup>−7</sup> in hot cores, 10<sup>−9</sup> in dark clouds and < 10<sup>−9</sup> in diffuse molecular gas [1, 2]. The  
5 methanol molecules observed in the ISM are not formed in the gas phase [3], but

---

<sup>1</sup>corresponding author

by successive hydrogenations of CO adsorbed on dust grains [4, 5]. Interstellar dust grains can be siliceous or carbonaceous, amorphous or crystallized, bare or covered by an ice mantle. Cosmic dust models [6] indicate that, in diffuse clouds, most of the carbon is found in carbonaceous grains and Polycyclic Aromatic Hydrocarbons (PAH). The proposed hydrogenation scheme for the solid state formation of methanol [5, 7, 8] is:



Methanol and the intermediate species HCO, CH<sub>3</sub>O and H<sub>2</sub>CO are thought to be precursors of complex organic molecules (COMs) on interstellar dust grains [9, 10, 11]. COMs have been detected in star forming regions at all steps of their evolution : molecular clouds, protostellar hot cores, envelopes, protoplanetary disks [12, 13, 14]. In the ISM, CO is formed in the gas phase and is accreted on the surfaces of grains in the dense and cold parts of molecular clouds [15] Andrews et al. [16] modeled physical conditions in PhotoDissociation Regions (PDR). The evolution of atom density, such as H, and molecule density, such as H<sub>2</sub> and CO, are reported as function of the extinction A<sub>v</sub> in the cloud. The density of CO molecules increases with A<sub>v</sub> while the density of H decreases with A<sub>v</sub>. Inside the molecular cloud, at high A<sub>v</sub>, the accretion of CO is high: an ice of CO recovers the grains. Before the formation of a CO ice, an intermediate density domain exists in the cloud, corresponding to lower CO accretion on the grain where the hydrogenation of CO can product complex molecules.

Many experimental and theoretical works have been devoted to the hydrogenation of CO and/or hydrogenated species reactions on surfaces [9, 17, 18, 19, 20, 21, 22, 23, 24, 25, 26] or in the gas phase [11, 20, 21, 22, 23, 24, 25, 27, 28]. Concerning H+CO reaction, Korchagina et al.[26] have performed a classical dynamics study on small water clusters (from 0-5 and 10 water molecules) using a SCC-DFTB (self-consistent-charge density functional tight-binding) approach. They have shown that on a cluster made of 10 water molecules, at 70K, the probability to form HCO adsorbed is 35% while the probability to form HCO which desorb in the gas phase is 5%. These results [26] are important because

35 the HCO radicals remaining adsorbed can be involved in further hydrogenation reactions leading to the methanol formation. Minisalle et al. [17] have investigated experimentally the  $\text{H} + \text{CO}$ ,  $\text{H} + \text{H}_2\text{CO}$  and  $\text{H} + \text{CH}_3\text{OH}$  reactions on an oxidized Highly Oriented Pyrolytic Graphite (HOPG) surface. From TPD (temperature programmed desorption) and RAIRS (reflection adsorption  
40 infrared spectrometer) experiments, they have concluded that, under their experimental conditions the methanol was formed by the hydrogenation of  $\text{H}_2\text{CO}$  but they did not observe methanol formation coming from CO hydrogenation. In DED experiments (During Exposure Desorption) they have measured chemical desorption of species corresponding to scheme 1 (eq. (1)). In a chemical  
45 desorption process, species formed on the substrate in exoergic reactions, can desorb using a fraction of the released chemical energy. For all the reactions and species, except CO and HCO, Minisalle et al. [17, 18] have shown that chemical desorption efficiency was low ( $< 5\%$ ). In an experimental and theoretical work, Butscher et al. [19] have investigated, by infrared spectroscopy, mass  
50 spectroscopy and DFT calculations, the HCO and  $\text{H}_2\text{COH}$  radicals produced after irradiation of  $\text{H}_2\text{CO}$  in gas rare matrices. They have shown that  $\text{CH}_2\text{OH}$  was the main intermediate species involved in the hydrogenation reaction of  $\text{H}_2\text{CO}$  leading to the formation of methanol.

In a QM/MM (quantum mechanics/molecular mechanics) treatment, Goumans  
55 et al. [20, 21] have calculated activation and reaction energies for methanol formation via the successive hydrogenations of CO in gas phase and adsorbed on negative charged defects of silicate surfaces. They have shown that, on silicate surface, the activation energies of  $\text{H} + \text{CO}$  and  $\text{H} + \text{H}_2\text{CO}$  reactions were reduced ( $-40\%$  and  $-15\%$  respectively) with respect to the gas phase values.  
60 These effects were related to the CO bond weakening and CO polarization increase in the adsorbed CO and  $\text{H}_2\text{CO}$  molecules. Surface effects on hydrogenation energies for reactions of scheme 1 (eq. (1)) were also obtained (see table 4). Rimola et al. [25] have investigated theoretically the  $\text{CO} + \text{H}$  and  $\text{H}_2\text{CO} + \text{H}$  reactions in the gas phase and adsorbed on water ices modeled by clusters with  
65 3, 18 and 32 water molecules. The activation energies of  $\text{H} + \text{CO}$  and  $\text{H} + \text{H}_2\text{CO}$

reactions, calculated at the DFT level for a cluster of 32 water molecules, were reduced ( $-18\%$  and  $-36\%$  respectively) with respect to the gas phase values. As in ref. [20, 25], these effects were related to the CO bond weakening and CO polarization increase due to H-bond formation between adsorbed CO and H<sub>2</sub>O  
70 molecules of the cluster. Surface effects on hydrogenation energies for reactions of scheme 1 (eq. (1)) were also obtained (see table 3). Using a numerical model of surface chemistry (GRAINNOBLE), the H<sub>2</sub>CO and CH<sub>3</sub>OH ice abundances have been simulated. All these works highlight the role of the nature of the surface [20, 25] in the methanol formation by successive hydrogenation reactions  
75 of CO.

The chemical pattern associated to hydrogenation reactions of CO adsorbed on a surface, is complex and implies reactions of scheme 1 (eq. (1)) but also abstraction reactions, for example  $\text{HCO} + \text{H} \rightarrow \text{CO} + \text{H}_2$ ,  $\text{H}_3\text{COH} + \text{H} \rightarrow \text{H}_2 + \text{CH}_2\text{OH}/\text{CH}_3\text{O}$  [22] or isomerization reactions, for example  $\text{CH}_3\text{O} \rightarrow \text{CH}_2\text{OH}$   
80 [17]. Goumans et al. [23] have shown that on surfaces covered by apolar ices or in the gas phase, the abstraction reaction  $\text{H} + \text{H}_2\text{CO} \rightarrow \text{H}_2 + \text{HCO}$  is predominant over the addition reaction  $\text{H} + \text{H}_2\text{CO} \rightarrow \text{H}_3\text{CO}$ . For some of these reactions, theoretical studies of Goumans et al. [20, 21, 23], Rimola et al. [25] and Korchagina et al. [26] have shown that on surfaces, activation energies are  
85 lowered with respect to the gas phase values. Nevertheless, barriers are still too large to be overcrossed in the cold ISM context. Goumans et al. [22, 23, 24] have shown that for the hydrogenated species of scheme 1 (eq. (1)), the tunneling effect has to be considered in hydrogenation or abstraction reactions at low temperature. A fraction of these hydrogenated species, formed on the grains in  
90 exoergic reactions, can be released in the gas phase through chemical desorption. In the ISM context, these processes are expected to contribute to gas phase molecular abundances. Consequently chemical desorption has been modeled for surface reactions leading to a single product and implemented in astrochemistry models developed for the ISM [4, 29, 30]. All these studies show the importance  
95 of the chemical desorption processes on the composition of the interstellar gas. These models rely on adsorption and hydrogenation reaction energies. More-

over Wakelam et al. [29] show the impact of these data on chemical desorption efficiency. There is an obvious need for consistent and complete data for hydrogenated CO species and for different substrates. **The present work is devoted to grain surface chemistry and to chemical desorption processes.** The aim of the present work is to provide absorption and hydrogenation energies of CO and related species on a bare graphene surface calculated with appropriate quantum chemical methods accounting for long range molecule-surface interactions.

In the present work, we study the interaction of isolated CO molecules adsorbed on a bare dust grain modeled by a graphene surface. **This model is relevant for low extinction values in PDR [16] as previously discussed and is expected to give upper limits for the chemical desorption probabilities.** The hydrogenated species, HCO, HCOH, H<sub>2</sub>CO, H<sub>3</sub>CO, H<sub>2</sub>COH, potentially involved in methanol formation have been considered. In the chemical network of the CH<sub>3</sub>OH formation, H addition reactions are in competition with H abstraction reactions. Present work is focussed on the chemical desorption induced by the energy released by hydrogenation reactions. In abstraction reactions, energy release is expected to be transferred to the relative motion of the products. Therefore the abstraction reactions are not considered in this work. Using Density Functional Theory (DFT) and a van der Waals functional, we have calculated the hydrogenation energies and obtained equilibrium geometries of each species in the gas phase and adsorbed on the substrate. Adsorption energies of each species on the graphene surface have been determined. In this work, we have considered an Eley-Rideal mechanism with an H atom coming from the gas phase. Finally, two chemical desorption models have been used to obtain the fractions of hydrogenated species that are released in the gas phase through chemical desorption. In the first part of this paper, the method and chemical reactions are presented. In the second part, results on the adsorption of isolated CO molecules on the graphenic surface are discussed. In the third part, results on the formation of hydrogenated species in the gas phase and adsorbed on the graphene surface are presented. In the fourth part, the results obtained with two different chemical desorption models [4, 17] are discussed. In the last part,

the summary and conclusion are presented.

## 2. Systems and Method

130 The successive hydrogenation reactions of CO molecules in the gas phase and adsorbed on a graphene surface have been investigated using the DFT method with a van der Waals functional for the description of the exchange-correlation terms. Ultrasoft pseudopotentials (PBE) are used. The kinetic energy cutoff is 50Ry for the wave function and 350Ry for the charge density  
135 and potential. The DFT calculations have been performed using the PWSCF code [31]. Calculations are carried out for a  $5 \times 5$  working cell using a  $4 \times 4$  k-points. For a  $3 \times 3$  working cell adsorption energies and hydrogenation energies are in the same order than for a  $5 \times 5$  working cell. The corresponding CO coverage rates are 4% and 10.5% for  $5 \times 5$  and  $3 \times 3$  working cells, respectively.  
140 Moreover, in the DFT calculations, the spin polarization scheme is used. The vdW functional used is the vdW-DF-cx [32, 33, 34]. The dipole moment of CO in the gas phase obtained with this functional is 0.116 Debye, in good agreement with the experimental value (0.11 Debye)[46] oriented towards the O atom.

In a previous work [35] on the adsorption at large distances (physisorption)  
145 of the coronene on a graphenic surfaces, we have shown that the vdW-DF-cx functional allows to reproduce physical and chemical adsorption characteristics.

For the adsorbed phase or the gas phase, the energies of hydrogenation reactions are calculated as :

$$\Delta_r E^{\text{surf or gas}} = E(\text{product/surf or gas}) - E(\text{reactant/surf or gas} + \text{H/gas}) \quad (2)$$

for  $\Delta_r E^{\text{surf or gas}} < 0$ , the reaction is exoergic and for  $\Delta_r E^{\text{surf or gas}} > 0$  the  
150 reaction is endoergic.

The first hydrogenation reactions involved in the methanol formation in the gas phase or in interaction with the graphene surface are:



The reaction (4) is endoergic ( $\Delta_r E^{\text{gas}} = +0.514\text{eV}$ ) (this work and Rimola et al. [25]) and is not considered in the following. The three different schemes of hydrogenation reactions leading to the methanol formation in the gas phase and in interaction with the graphene surface are:



This scheme corresponds to the complete hydrogenation of the C atom followed by the hydrogenation of the O atom. This hydrogenation scheme is known to be energetically favorable (lowest addition barriers) and is usually considered in the literature [5, 7, 8]. To account for the experimental observation of  $\text{H}_2\text{COH}$  [19] 3 mechanisms are possible: the isomerization of  $\text{H}_3\text{CO}$  as proposed by Minisalle et al. [18], the abstraction reaction on methanol [21], or the hydrogenation of  $\text{H}_2\text{CO}$  [22] and  $\text{HCOH}$ . Previous work of Goumans [21] shows that, the abstraction barriers are  $0.377\text{eV}$  for the  $\text{H} + \text{H}_3\text{COH} \rightarrow \text{H}_2 + \text{CH}_2\text{OH}$  reaction and  $0.572\text{eV}$  for the  $\text{H} + \text{H}_3\text{COH} \rightarrow \text{H}_2 + \text{CH}_2\text{O}$  reaction, in the gas phase. Therefore they [21] conclude that at low temperatures, the tunneling should be important for these abstraction reactions. In the gas phase, for  $\text{H} + \text{H}_2\text{CO} \rightarrow \text{CH}_3\text{O}$  reaction, the addition barrier is  $0.105\text{eV}$  in Rimola et al. [25] and  $0.139\text{eV}$  in Song et al. [28]. For  $\text{H} + \text{H}_2\text{CO} \rightarrow \text{CH}_2\text{OH}$  reaction, the addition barrier is in  $0.34\text{eV}$  for Rimola et al. [25] and  $0.41\text{eV}$  in Song et al. [28]. All these barriers [21, 25, 28] are high and tunneling effects are expected to play an important role in the chemical reactions. Consequently, in the present work, we have also considered the following alternative hydrogenation schemes:



where the hydrogenation of  $\text{H}_2\text{CO}$  leads to the formation of the radical  $\text{H}_2\text{COH}$  and,



where the hydrogenation of  $\text{HCO}$  leads to the formation of hydroxymethylene ( $\text{HCOH}$ ). Note that  $\text{HCOH}$  has two conformers which are considered in this

work: the cis form (reactions 7 and 8) and the trans form (reactions 7' and 8').

180 For reactions (1), (3), (5) and (8), we have not calculated the barriers. Indeed, the vdW-DF-cx functional is known to underestimate the barriers for hydrogenation reactions [36]. Moreover, previous works [21, 25, 28] show that addition and abstraction barriers are high and that the tunneling effect is predominant.

### 185 **3. CO adsorption on a graphene surface**

For the adsorption of an isolated CO molecule on a graphene surface, three sites have been investigated (figure 1): the top (T) site, above a carbon atom of the surface, the hollow (H) site, above the center of a hexagonal ring of the graphene surface, and the bridge (B) site, above the middle of a carbon-carbon  
190 bond of the surface. Two different adsorption geometries have been studied : with the CO molecule parallel or perpendicular to the surface. For the parallel geometry, three different orientations have been considered : with C or O above a top or a hollow site, and with the middle of the CO bond above the bridge site. For the perpendicular geometry, two different orientations have been considered:  
195 with C or O atoms pointing towards the surface. The corresponding energies and geometries are summarized in table 1. The adsorption energy of CO on the graphene surface is defined as:

$$\Delta E^{\text{ads}} = E(\text{CO/graphene}) - E(\text{CO}_{\text{gas}} + \text{graphene}) \quad (8)$$

Our results show a clear geometrical dependence: the adsorption energies vary from  $-0.163\text{eV}$  to  $-0.155\text{eV}$  for parallel geometries, and from  $-0.124\text{eV}$  to  
200  $-0.114\text{eV}$  for perpendicular geometries. On the other hand, our results show very weak site and orientation dependence : the graphene surface is not corrugated. Moreover, for all geometries, the typical CO-surface equilibrium distance is  $3.2\text{\AA}$ .

The strongest physisorption energy,  $\Delta E^{\text{ads}} = -0.163\text{eV}$ , is obtained for the  
205 hollow site, with CO parallel to the surface and the O atom above the hol-

low site. This value and the equilibrium geometry are in good agreement with Zhang et al. [37] who obtained an adsorption energy of  $-0.120\text{eV}$  in a DFT calculation with the LDA approximation. Several theoretical studies on the CO adsorption on a graphene surface using DFT calculations at the GGA level with the PBE functional have been performed [38, 39]. In these studies, adsorption energies vary from  $-0.008\text{eV}$  to  $-0.016\text{eV}$  and the corresponding CO-graphene equilibrium distances from  $3.720$  to  $3.768 \text{ \AA}$ . The underestimation of adsorption energies and overestimation of equilibrium distances are a well-known drawback of DFT GGA calculations which cannot account for weak van der Waals interactions. Recent calculations of Wilson et al. [40] on the adsorption of CO on coronene using coupled cluster calculations and on circumcoronene using the DFT calculations with the B97D functional have shown that there are no preferential adsorption sites but that the orientation of the molecule with respect to the coronene/circumcoronene is important as obtained in present work.

In the present work, the bond length of the adsorbed CO remains very close to the gas phase value,  $1.140\text{\AA}$ , whatever the adsorption site and the geometry; as expected for a defectless graphene surface, the adsorbed CO molecules are unperturbed and are weakly interacting with the surface i.e. the CO molecules are physisorbed on the graphene. In order to accurately describe molecular physisorption on graphenic surfaces with DFT calculations, one should include van der Waals interactions as we have done.

#### 4. Hydrogenation reactions : from CO to methanol in the gas phase and adsorbed on a graphene surface

The energies and equilibrium geometries of hydrogenated-CO species involved in hydrogenation schemes 1, 2 and 3 have been calculated at the DFT vdW-DF-cx level, in the gas phase, and for the deposited phase, starting with a CO molecule adsorbed at the hollow site on the graphene. The hydrogenation energies for the deposited phase,  $\Delta_r E^{\text{surf}}$ , for the gas phase,  $\Delta_r E^{\text{gas}}$ , and the adsorption energies,  $\Delta E^{\text{ads}}$  are presented in table 2.

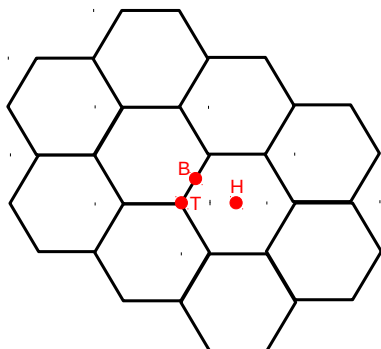
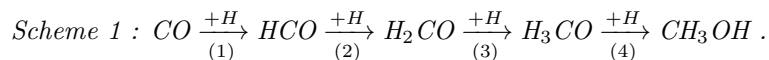


Figure 1: Adsorption sites of CO on a graphene surface. H: Hollow, B: Bridge, T: Top.

235 The hydrogenation energies are defined in equation (2). For a given reaction, the adsorption energy of the product  $\Delta E^{\text{ads}}(\text{product})$  is related to the difference in the hydrogenation energies on the surface and in the gas phase and to the adsorption energy of the reactant  $\Delta E^{\text{ads}}(\text{reactant})$ :

$$\Delta E^{\text{ads}}(\text{product}) = \Delta E^{\text{ads}}(\text{reactant}) + \Delta_r E^{\text{surf}} - \Delta_r E^{\text{gas}} \quad (9)$$

240 Our results on the hydrogenation reactions in the gas phase and in the adsorbed phase are summarized in table 2 and figure 3. One of main results is that the hydrogenation energies of each species are similar in the gas phase and in the adsorbed phase.



245 For scheme 1, our gas and adsorbed phase hydrogenation energies are compared with results obtained by Rimola et al. [25], and by Goumans et al. [20] in table 3. As one can see, for the gas phase reactions, the energies obtained in the three works are in good agreement. Hydrogenation energies for the gas phase reactions 1, 3 are in the range  $-0.82\text{eV}$  to  $-1.68\text{eV}$ , these reactions are closed-shell plus radical reactions. The exoergicities obtained, correspond to an energy  
250 balance between the formation of a CH bond and the weakening of the CO triple bond (reaction 1) or of the CO double bond (reaction 3). Reactions 2 and 4 are

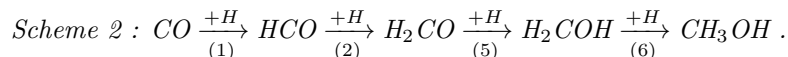
CO <sub>geom.</sub> / CO <sub>orient.</sub>	Top site			Hollow site			Bridge site		
	$\Delta E^{ads}$ (eV)	d <sub>C</sub> (Å)	d <sub>O</sub> (Å)	$\Delta E^{ads}$ (eV)	d <sub>C</sub> (Å)	d <sub>O</sub> (Å)	$\Delta E^{ads}$ (eV)	d <sub>C</sub> (Å)	d <sub>O</sub> (Å)
/ C <sub>above</sub> site	-0.157	3.142	3.252	-0.155	3.209	3.238	n.c	n.c	n.c.
/ O <sub>abovesite</sub>	-0.155	3.210	3.273	-0.163	3.125	3.275	n.c	n.c	n.c.
/ CO <sub>middle</sub> bond	n.c.	n.c	n.c	n.c	n.c	n.c	-0.158	3.138	3.332
⊥ / C <sub>towards</sub> surf.	-0.115	3.350	4.490	-0.124	3.167	4.30	-0.116	3.339	4.476
⊥ / O <sub>towards</sub> surf.	-0.115	4.353	3.213	-0.117	4.172	3.031	-0.114	4.280	3.138

Table 1: Adsorption energies of CO on a top, hollow and bridge sites of the graphene (figure 1). d<sub>C</sub> and d<sub>O</sub> are the distances to the graphenic surface. CO bond length is 1.140 Å whatever the site and the geometry. n.c : not calculated. CO<sub>geom.</sub> indicates the geometry of CO : parallel or perpendicular. CO<sub>orient.</sub> indicates the orientation of CO on the graphene surface.

radical plus radical reactions, they correspond to the formation of a CH bond (reaction 2) or of an OH bond (reaction 4), the corresponding exoergicities are in the range  $-3.69\text{eV}$  to  $-4.72\text{eV}$ . The results on the adsorbed phase reported in the table 3 show the effect of the surface on the hydrogenation energies. Consequently, for negatively charged defects on a silicate surface [20, 21], a strong surface effect on hydrogenation energies is obtained. This effect is weaker on water ice (modeled by a cluster of 32 water molecules in the work of Rimola et al. [25] or by a cluster of 10 water molecules in the work of Korchagina et al. [26]) and on a graphenic surface (present work). This effect is related to adsorption energies of reactants and products (see eq.(9)). Indeed, for a given hydrogenation reaction, if the adsorption energies of reactant and product are similar, the hydrogenation energies for the gas phase and the adsorbed phase are expected to be similar. Conversely, if the adsorption energy of the product is stronger (weaker) than the adsorption energy of the reactant, the hydrogenation energy is expected to be higher (smaller) for the adsorbed phase. Therefore, on a graphenic surface, exoergicity of reaction 3 is enhanced and exoergicity of reaction 4 is reduced. Indeed, the adsorption energy of the methoxy radical (CH<sub>3</sub>O) is the strongest :  $-0.337\text{eV}$ , while adsorption energies of formaldehyde

(CH<sub>2</sub>O) and methanol are respectively  $-0.212\text{eV}$  and  $-0.247\text{eV}$ .

Our results (table 2) shows that the adsorption energies of the species on the graphene surface are important and vary between  $-0.175\text{eV}$  for HCO and  $-0.337\text{eV}$  for CH<sub>3</sub>O. Several experimental [42, 43] or theoretical [41, 44] studies  
275 have been performed on adsorption of formaldehyde and methanol on different surfaces, the corresponding adsorption energies values are presented in table 4. Chi and Zao [41] have performed a DFT-GGA study of the formaldehyde adsorption on a graphene surface, but DFT-GGA does not account for vdW interactions and the corresponding adsorption energy ( $-0.083\text{eV}$ ) is underestimated.  
280 The formaldehyde adsorption energy on graphene (present work:  $-0.212\text{eV}$ ) is of the same order and weaker than experimental values obtained on an olivine [42] and a water ice surface [42]. Concerning methanol adsorption, E. Schröder [44] has performed a DFT calculation with a vdW-DF functional on a graphene surface. This work shows that adsorption energies increase with the methanol  
285 coverage rate on the surface, in agreement with experimental work of Bolina et al.[43]. At a low coverage, the adsorption energy is  $-0.212\text{eV}$  in good agreement with the present work value:  $-0.247\text{eV}$ .



290 For the alternative hydrogenation scheme 2 proposed in present work, gas phase exoergicities of reactions 1 and 5 (closed-shell plus radical reactions) are  $-1.27\text{eV}$  and  $-1.68\text{eV}$  respectively. For the reaction 5, the exoergicity correspond to an energy balance between the formation of an OH bond and the weakening of the CO double bond. This latter value is in good agreement with  
295 the value obtained by Rimola et al.[25]:  $-1.71\text{eV}$ . For reactions 2 and 6, (radical plus radical reactions) gas phase exoergicities are  $-4.05\text{eV}$  and  $-4.37\text{eV}$ . Whatever the reaction, the exoergicities in the adsorbed phase are of the same order as in the gas phase. For this scheme, the surface effect on exoergicities is small. Indeed, the adsorption energy of the hydroxymethyl radical, H<sub>2</sub>COH on  
300 graphene is close to adsorption energies of formaldehyde and methanol. More-

over, our results confirm that the isomer  $\text{H}_2\text{COH}$  (obtained by the scheme 2) is more stable than  $\text{H}_3\text{CO}$  (obtained by the scheme 1) (see figure 3) as is well known [25, 45]

The total energies of CO-hydrogenated species adsorbed on the graphene surface are shown in figure 3. The methanol molecules formed in scheme 1 and 2 correspond to slightly different total energy levels:  $-11.422\text{eV}$  and  $-11.446\text{eV}$ , respectively. These energy differences are related to different final conformations and orientations of the methanol molecules on the graphene surface, as illustrated in figure 2. Similarly, the corresponding adsorption energies for the methanol obtained with different conformations in hydrogenation schemes 1 and 2 differ:  $-0.247\text{eV}$  and  $-0.263\text{eV}$  respectively: the graphene surface is weakly corrugated.

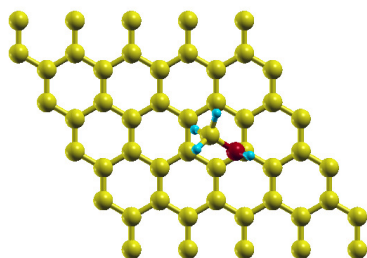


In the scheme 3, the hydroxymethylene ( $\text{HCOH}$ ) can be formed in a cis (reaction 7) or a trans (reaction 7') conformation. In the adsorbed phase, the hydrogenation energies corresponding to the formation of these species are  $-1.631\text{eV}$  and  $-1.867\text{eV}$ , respectively. The cis and trans  $\text{HCOH}$  species are located at  $+2.456\text{eV}$  and  $+2.222\text{eV}$  eV with respect to the stablest isomer  $\text{H}_2\text{CO}$ . In the gas phase, the results are of the same order. These values are in good agreement with calculated energy levels obtained with high level ab-initio correlated calculations [46]:  $+2.444\text{eV}$  and  $+2.337\text{eV}$ , respectively. Consequently, reactions 7 and 7' are much less exoergic than reaction 2. For the cis and trans  $\text{HCOH}$ , adsorption energies on graphene are greater than for formaldehyde:  $-0.221\text{eV}$ ,  $-0.263\text{eV}$  and  $-0.212\text{eV}$ , respectively. Reactions 8 and 8' correspond to hydrogenation of cis and trans  $\text{HCOH}$ , producing  $\text{CH}_2\text{OH}$  in slightly different conformations and orientations on the graphenic surface. As discussed in the previous paragraph for methanol, corresponding total energies and adsorption energies differ for the  $\text{H}_2\text{COH}$  species formed on the graphene surface by reaction 8 or 8', see table 2 and fig. 3. A weak corrugation of the surface is observed. Finally,

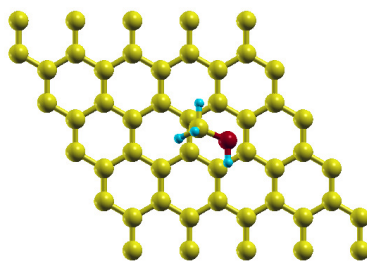
in a similar way, the hydrogenation reactions of the  $\text{H}_2\text{COH}$  species (reactions 6') produce methanol molecules with slightly different conformations and orientations (see Fig. 2) on the graphene surface. In scheme 3 as in scheme 2, the surface effect on exoergicities is small and the largest exoergicity enhancement  
335 is obtained for reaction 7', corresponding to the formation of the trans-HCOH species.

In order to estimate the Zero-point energy (ZPE) corrections to the adsorption energies, we have calculated the one dimensional potential energy curve for the adsorption of CO on the hollow site of the graphene (see table 1). The cor-  
340 responding ZPE correction obtained with the Numerov's algorithm is 0.006eV. Considering this weak value, the ZPE corrections are not included in present work.

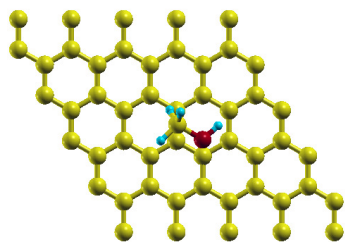
As a conclusion of this section, all the considered reactions in this work are exoergic and all the corresponding hydrogenated-CO species are physisorbed  
345 on the graphene surface. The adsorption energies are between  $-0.175\text{eV}$  and  $-0.337\text{eV}$  eV and at low temperature, thermal desorption of all these species is not expected to be an efficient process.



a)



b)



c)

Figure 2: Methanol molecule on the surface via: a) scheme 1, b) scheme 2, c) scheme 3

Reactants	Reaction	Product	$\Delta_r E^{\text{surf}}$ (eV)	$\Delta_r E^{\text{gas}}$ (eV)	$\Delta E^{\text{ads}}$ (eV)
H+CO	1	HCO	-1.282	-1.270	-0.175
HCO+H	2	H <sub>2</sub> CO	-4.087	-4.050	-0.212
H <sub>2</sub> CO+H	3	H <sub>3</sub> CO	-1.425	-1.324	-0.337
H <sub>3</sub> CO+H	4	H <sub>3</sub> COH	-4.628	-4.718	-0.247
H <sub>2</sub> CO+H	5	H <sub>2</sub> COH	-1.690	-1.680	-0.246
H <sub>2</sub> COH+H	6	H <sub>3</sub> COH	-4.384	-4.367	-0.263
HCO+H	7	cis-HCOH	-1.631	-1.584	-0.221
cis-HCOH+H	8	H <sub>2</sub> COH	-4.133	-4.147	-0.207
H <sub>2</sub> COH+H	6'	H <sub>3</sub> COH	-4.382	-4.367	-0.222
HCO+H	7'	trans-HCOH	-1.867	-1.779	-0.263
trans-HCOH+H	8'	H <sub>2</sub> COH	-3.961	-3.951	-0.273
H <sub>2</sub> COH+H	6'	H <sub>3</sub> COH	-4.326	-4.364	-0.235

Table 2: Hydrogenation energies of species adsorbed on the graphene surface ( $\Delta_r E^{\text{surf}}$ ) and in the gas phase ( $\Delta_r E^{\text{gas}}$ ).  $\Delta E^{\text{ads}}$  are the adsorption energies of the molecules on the graphene surface. Black color : reaction (1) and (2) for each scheme. Blue color: scheme 3. Red color: scheme 1. Green color: scheme 2.

Reactions	Silicate surf. [20] $\Delta_r E^{\text{surf}}$ ( $\Delta_r E^{\text{gas}}$ ) (eV)	Water ice surf. [25] $\Delta_r E^{\text{surf}}$ ( $\Delta_r E^{\text{gas}}$ ) (eV)	Graphene surf. (this work) $\Delta_r E^{\text{surf}}$ ( $\Delta_r E^{\text{gas}}$ ) (eV)
CO+H $\xrightarrow{(1)}$ HCO	-1.37 (-0.82)	-1.15 (-1.01)	-1.28 (-1.27)
HCO+H $\xrightarrow{(2)}$ H <sub>2</sub> CO	-3.48 (-3.69)	/	-4.09 (-4.05)
H <sub>2</sub> CO+H $\xrightarrow{(3)}$ H <sub>3</sub> CO	-1.31 (-1.07)	-1.50 (-1.52)	-1.42 (-1.32)
H <sub>3</sub> CO+H $\xrightarrow{(4)}$ CH <sub>3</sub> OH	-4.67 (-4.19)	/	-4.63 (-4.72)
H <sub>2</sub> CO+H $\xrightarrow{(5)}$ H <sub>2</sub> COH	/	(-1.71)	-1.69 (-1.68)

Table 3: Calculated hydrogenation energies on a silicate surface [20], on a cluster of 32 water molecules[25], and on graphene (this work) for reactions (1), (2), (3), (4) and (5). Values in parentheses correspond to the gas phase reactions.

Species	Graphene	HOPG	Olivine	Water ice
H <sub>2</sub> CO	-0.083 <sup>a</sup> , [41] -0.212 <sup>this work</sup>	/	-0.321 <sup>b</sup> , [42]	-0.281 <sup>b</sup> , [42]
CH <sub>3</sub> OH	-0.214 <sup>a</sup> , [44] -0.247 <sup>this work</sup>	-0.342 <sup>b</sup> , [43]	/	/

Table 4: Adsorption energies of formaldehyde and methanol in eV for different surfaces. a: calculated values, b: experimental values from TPD experiments.

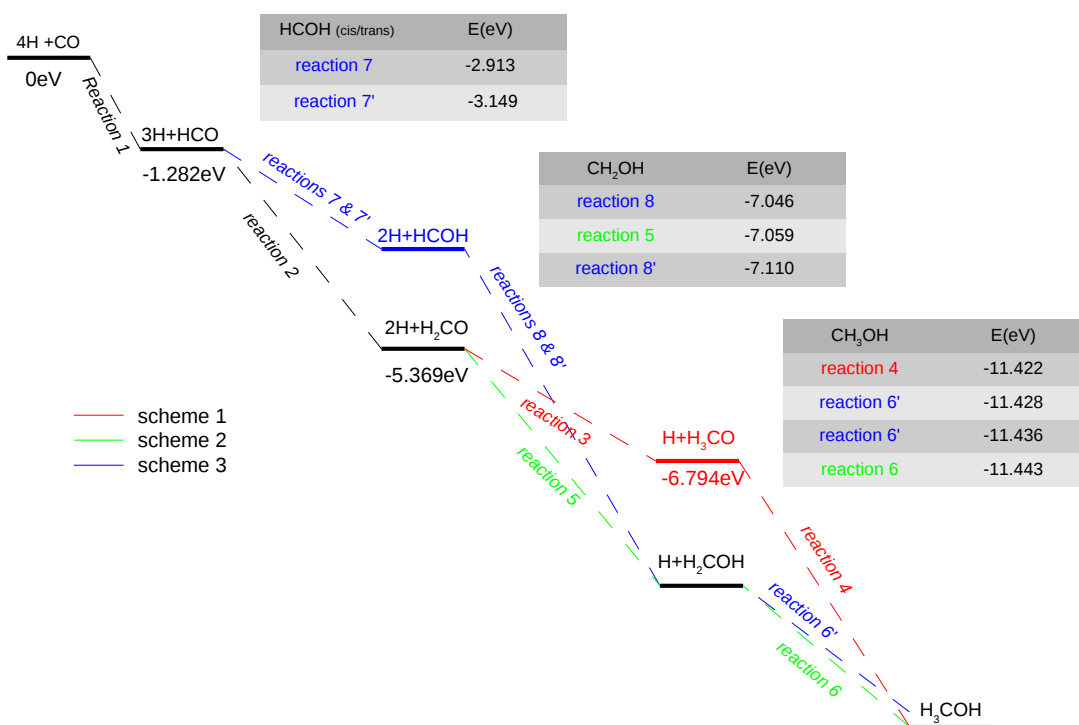


Figure 3: Schematic energy level diagram of isolated CO-hydrogenated species adsorbed on a graphene surface. Origin of energy : CO<sub>adsorbed</sub> + 4H<sub>gas</sub>. Numerical values are reported in the tables.

## 5. Chemical Desorption

The Chemical Desorption (CD) process requires some exoergic reactions. In  
350 this process, a fraction of the chemical energy released by the formation reaction  
is transferred to the molecules and molecules can desorb from the surface. Two  
CD models have been proposed by Garrod et al. [4] and Minisalle et al. [18]  
for surface reactions producing single species (i.e.  $A + B \rightarrow C$  reactions). For a  
given reaction, the CD probability represents the fraction of molecules formed  
355 on the surface that are released in the gas phase.

*Rice-Ramsperger-Kessel model.*

In the CD model proposed by Garrod et al. [4], CD probability is calculated  
using the model of Rice-Ramsperger-Kessel [47, 48] (named RRK model).

360 In the RRK model, the probability for an energy  $E$  to be located in the  
molecule-surface bond is:

$$P = \left(1 - \frac{E_b}{E_{react}}\right)^{s-1} \quad (10)$$

where  $E_b$  is the adsorption energy of the product,  $E_{react}$  is the reaction formation  
energy,  $s$  is equal to  $3N - 5$  and  $N$  is the number of atoms in the molecule.  
The fraction of molecules released in the gas phase by chemical desorption is  
365 expressed as:

$$f = \frac{aP}{1 + aP} \quad (11)$$

where  $a$  is a parameter modeling the competition between desorption and energy  
loss to the surface. Following Garrod et al.[4] we have used the value  $a = 0.03$   
for all the CO-hydrogenated species formed on the graphene surface.

*Minisalle et al. model.*

370

In the CD model proposed by Minisalle et al. [18] (named MDCH model in ref.[29]), the CD probability is :

$$f = \exp\left(-\frac{E_b}{\varepsilon\Delta H/N}\right) \quad (12)$$

where  $N$  is the number of degrees of freedom of the produced molecules and  $\Delta H$  is the enthalpy of reaction.  $\varepsilon = \frac{(M-m)^2}{(M+m)^2}$ , where  $m$  is the molecule mass and  $M$  the effective mass of the surface. Assuming an elastic collision,  $\varepsilon$  is the fraction of the kinetic energy left in the molecule. In their work, Minisalle et al. [18] concluded that  $M = 120$  a.m.u was the best value for reproducing their experimental CD results obtained on a bare oxidized HOPG surface. In the present work, we have retained  $M = 120$  a.m.u. in order to compare our results with results of ref. [18]. In the MDCH model, the chemical desorption is treated as an elastic collision between the formed molecule and the surface.

These models should be relevant for CD on a graphene surface. Indeed, the energy transfer between the molecule and a surface is expected to be weaker for a bare graphenic surface than for silicated or ice-covered surfaces. Moreover, molecular species are physisorbed on the graphene surface and adsorption energies are weak. Finally, in the case of isolated molecules, energy transfer to adjacent molecules on the surface is also expected to be small. In this way, CD probabilities calculated in present work should represent upper limits.

### Results and discussion.

For reactions considered in the present work, the CD probabilities calculated with the RRK and the MDCH models, are reported in table 5.

In the RRK model, the CD probabilities are weak, whatever the molecules. Note that in this model, see eq.(11), the value of the parameter  $a$  gives the upper limit for the CD probabilities. The RRK model does not distinguish between reactions: for example, the reactions  $\text{H}_3\text{CO}+\text{H} \xrightarrow{(4)} \text{H}_3\text{COH}$  and  $\text{H}_2\text{COH}+\text{H} \xrightarrow{(6)} \text{CH}_3\text{OH}$  correspond to the methanol formation with different exoergcities and

adsorption energies (see table 2), but resulting CD probabilities are similar.  
400 This feature has already been pointed out by Wakelam et al.[29] and Minisalle  
et al. [18]. In present work, the highest CD probability is obtained for the  
formaldehyde (2.13%), and the lowest for the methoxy radical,  $\text{CH}_3\text{O}$  (0.26%).

In the MDCH model, the CD probabilities depend much more on reactions  
than in the RRK model. For  $\text{H}_3\text{CO}$  (produced in reaction 3),  $\text{H}_2\text{COH}$  (produced  
405 in reaction 5), cis and trans-HCOH (produced in reactions 7 and 7'), CD proba-  
bilities are weak ( $\leq 1\%$ ) and are smaller than the RRK ones. The corresponding  
hydrogenation reactions are characterized by low exoergicities ( $\leq 1.867\text{eV}$ ) and  
high adsorption energies ( $\geq 0.221\text{eV}$ ), in absolute values, see table 2. For the  
others species CD probabilities are greater than the RRK ones. For  $\text{H}_2\text{CO}$  (pro-  
410 duced in reaction 2) and  $\text{H}_2\text{COH}$  (produced in reaction 8 via the hydrogenation  
of the cis-HCOH) MCDH CD probabilities are high ( $\geq 10\%$ ). The correspond-  
ing hydrogenation reactions are characterized by high exoergicities ( $\geq 4.087\text{eV}$ )  
and low adsorption energies ( $\leq 0.212\text{eV}$ ), in absolute values, see table 2.

Reactions	Molecule formed	RRK model [4] a=0.03 CD (%)	MDCH model [18] M=120 a.m.u CD (%)
CO+H	HCO	1.89	3.71
HCO+H	cis-HCOH	1.23	1.09
cis-HCOH+H	H <sub>2</sub> COH	1.85	11.50
H <sub>2</sub> COH	H <sub>3</sub> COH	1.58	6.58
HCO+H	trans-HCOH	1.19	0.91
trans-HCOH+H	H <sub>2</sub> COH	1.55	5.09
H <sub>2</sub> COH	H <sub>3</sub> COH	1.51	5.41
HCO+H	H <sub>2</sub> CO	2.13	17.74
H <sub>2</sub> CO+H	H <sub>2</sub> COH	0.72	0.186
H <sub>2</sub> COH+H	H <sub>3</sub> COH	1.45	4.61
H <sub>2</sub> CO+H	H <sub>3</sub> CO	0.26	0.004
H <sub>3</sub> CO+H	H <sub>3</sub> COH	1.52	5.69

Table 5: Chemical Desorption probabilities calculated with the RRK model [4] and the MDCH model [18] as function of chemical reactions.

In the ISM, CO-hydrogenated species formed on the graphenic surface by successive hydrogenation reactions, albeit physisorbed, cannot undergo thermal desorption processes. Nevertheless, our calculations show that, whatever the CD model, the formaldehyde molecule has the highest CD probability and that MCDH CD probability for H<sub>2</sub>COH resulting from hydrogenation of cis-HCOH is also high. Consequently, these species, if formed on the grains, are expected to show high gas phase abundances due to chemical desorption processes. Moreover present work shows that in the gas phase, hydroxymethyl radicals (CH<sub>2</sub>OH) should come specifically from chemical desorption due to the hydrogenation of deposited cis-HCOH.

The methoxy radical, CH<sub>3</sub>O, has been detected in the ISM [49], while the hydroxymethyl radical, CH<sub>2</sub>OH, which is the stablest isomer, has not yet been

detected [50]. But Butscher et al. [19], in experimental work, show that  $\text{CH}_2\text{OH}$  is an intermediate species implied into the methanol formation. The role of the intermediate  $\text{CH}_2\text{OH}$  is still under debate. Our results show that adsorption energy of the  $\text{CH}_3\text{O}$  species is quite high and that the CD probability of  $\text{CH}_3\text{O}$  is negligible. The methoxy radicals are expected to be condensed on ISM grains and  $\text{CH}_3\text{O}$  species in the ISM gas phase cannot come from reaction 3 and are formed by other mechanism [22]. Conversely, the MCDH CD probabilities for  $\text{CH}_2\text{OH}$  radicals are high (5% for the radical formed by hydrogenation of trans-HCOH and 11.5% for the radical formed by hydrogenation of cis-HCOH). Relatively high gas phase abundances should be observed for these species. Nevertheless, these very reactive species can be involved in many surface chemical reactions, in competition with reactions considered in the present work.

For the three hydrogenation schemes considered, the CD probabilities for methanol obtained in the MCDH model amount to 5% and are higher than the RRK ones. Wakelam et al. [29], have modeled adsorption energies on water ice and have tested the RRK and MCDH CD models. In their work, MCDH CD probabilities for methanol and other species are low and smaller than the RRK ones. This feature is related to the high values of adsorption energies derived for water ice in their work (HCO: -0.207 eV,  $\text{H}_2\text{CO}$ : -0.388eV,  $\text{CH}_3\text{O}$ :-0.379eV, CH-2OH: -0.379eV and  $\text{CH}_3\text{OH}$ : -0.431eV). Finally, Wakelam et al. [29] conclude that resulting weak CD probabilities cannot account for observed  $\text{CH}_3\text{OH}$  abundances in cold cores. Our results show that methanol CD probabilities are higher on bare graphenic than ice surfaces [29]. Moreover, on the graphene surface, the radical species  $\text{CH}_3\text{O}$ , cis and trans-HCOH have very weak CD probabilities, are expected to be physisorbed on the surface and to be involved in surface chemical reactions.

## 6. Summary & Conclusion

In this work, DFT with a VdW functional have been used to calculate the hydrogenation and adsorption energies of isolated CO and related species on a

455 graphene surface.

Three scenario producing methanol have been considered. The originality of this work is to consider scenarios with intermediate molecules as CH<sub>2</sub>OH, trans and cis-HCOH. The hydrogenation of cis-HCOH and trans-HCOH produce CH<sub>2</sub>OH with different orientations on the surface and a small difference in the  
460 relative energies: the surface is weakly corrugated. Moreover, our DFT results show that CH<sub>3</sub>O has a large adsorption energy on the surface and that the chemical desorption probability is very small: if CH<sub>3</sub>O is formed on the surface, it is condensed on the surface and can interact with others atoms or molecules.

In the gas phase and on a cluster of 3 water molecules, Rimola et al. [25]  
465 have shown that the hydrogenation barrier for the formation of the methoxy radical, CH<sub>3</sub>O, is much smaller (0.10eV) than the barrier for the formation of the hydroxymethyl radical, CH<sub>2</sub>OH, (0.34eV). Thus at low temperature, the formation probability of CH<sub>2</sub>OH is smaller than the formation probability of CH<sub>3</sub>O by hydrogenation of CH<sub>2</sub>O. In an experimental study, Butscher et al.  
470 [19] have demonstrated that on water ices, H<sub>2</sub>COH was the main intermediate in the H<sub>2</sub>CO to CH<sub>3</sub>OH hydrogenation process. Minisalle et al.[17] have experimentally investigated the hydrogenation of CO on Oxydized HOPG surfaces. They have proposed the following scheme:



But Xu et al. [45], in a quantum chemical ab-initio CCSD(T) calculation, have  
475 obtained an energy barrier of 1.28eV for the isomerization reaction from CH<sub>3</sub>O to CH<sub>2</sub>OH in the gas phase. Thus the formation barriers are smaller than the isomerization barriers. Consequently, at low temperatures, the isomerization processes should not be a favorable way to produce CH<sub>2</sub>OH compared to hydrogenation reactions. In the present work, we consider the formation of  
480 CH<sub>2</sub>OH via the hydrogenation of cis-HCOH and trans-HCOH (reaction 8 and 8'). In a theoretical IR study of trans and cis HCOH in the gas phase, Koziol et al.[51] have performed ab-initio CCSD(T)/aug-cc-pVTZ calculations and have found energy barriers for the isomerization of formaldehyde to trans-HCOH

and for the isomerization of trans-HCOH to cis-HCOH of +3.7eV and +0.96eV,  
485 respectively. Considering these high isomerization barriers, the alternative hy-  
drogenation scheme 3 in which the H<sub>2</sub>COH, cis and trans-HCOH species are  
formed by direct hydrogenation reactions should be relevant. In the present  
work, this scheme is studied in detail and show that if CH<sub>2</sub>OH is formed on the  
surface via the hydrogenation of trans-HCOH on the graphene surface then it  
490 has a large probability to desorb in the gas phase.

For all these species, chemical desorption probabilities have been calcu-  
lated with two different models. Whatever the CD models and hydrogena-  
tion scenarios, the CD probabilities for the methanol molecules amount to 5%.  
Consequently, on a bare graphene surface, methanol molecules should be ph-  
495 ysisorbed, and chemical desorption processes are expected to contribute weakly  
to gas phase abundances. The species that have the highest CD probabilities  
are formaldehyde, H<sub>2</sub>CO, and for hydroxymethyl radicals, H<sub>2</sub>COH: for these  
species, chemical desorption processes are expected to enhance gas phase abun-  
dances.

## 500 Acknowledgements

S.M. thanks Denis Hagebaum-Regnier and Stéphanie Cazaux for useful dis-  
cussion.

- [1] Liszt H.S., Pety J., Lucas R. *A&A* 486, 493 (2008)
- [2] Wirström E.S., Geppert W.D., Hjalmarsen A, Persson C.M., Black J.H.,  
505 Bergman P., Millar T.J., Hamberg M., Vigren E. *A&A* 533 A24 (2011)
- [3] Herbst E., van Dishoeck E. *Annu. Rev. Astron. Astrophys.* 47 427-480  
(2009)
- [4] Garrod R.T., Wakelam V., Herbst E., *A&A* 467 1103 (2007)
- [5] Watanabe N., Shiraki T., Kouchi A., *Astrophys. J.* 588 L121-L124 (2003)
- 510 [6] Ehrenfreund P., Cami J. *Cold Spring Harb. Perspect. Biol.* 2 12 (2014)

- [7] Hiraoka K., Sato T., Sato S., Sogoshi N., Yokoyama T., Takashima H., Kitagawa S., *Astrophys. J.* 577 265-270 (2002)
- [8] Tielens A.G.G.M., Hagen W., *A&A* 114 245 (1986)
- [9] Theulé P., Duvernay F., Danger G., Borget F., Bossa J.B., Vinogradoff V., Mispelaer F., Chiavassa T. *Adv. Space Res.* 52 8 1567-1579 (2013)
- 515 [10] Caselli P., Ceccarelli C. *Astron. Astrophys. Rev.* 20 56 1-68 (2012)
- [11] Fedoseev G., Cuppen H.M., Ioppolo S., Lamberts T., Linnartz H. *MNRAS* 448 1288-1297 (2015)
- [12] Bottinelli, S., Ceccarelli, C., Williams, J. P., Le floch, B. *A&A*,463, 601  
520 (2007)
- [13] Vastel, C., Ceccarelli, C., Le floch, B., & Bachiller, R. , *ApJL*,795, L2 (2014)
- [14] Öberg K.I., Guzmán V.V., Furuya K. et al. *Nature* 520 198 (2015)
- [15] Chuang K.J., Fedoseev G., Ioppolo S., van Dishoeck E.F., Linnartz H.,  
525 *MNRAS* 455 1702 (2016)
- [16] Andrews H., Candian A., Tielens A.G.G.M *A&A* 595 A23 (2016)
- [17] Minisalle M., Moudens A., Baouche S., Chaabouni H., Dulieu F., *MNRAS* 458 2953 (2016)
- [18] Minisalle M., Dulieu F. Cazaux S., Hocuk S., *A&A* 585 A24 (2016)
- 530 [19] Butscher T, Duvernay F., Theulé P., Danger Y., Carissan Y., Hagebaum-Regnier D., Chiavassa T., *MNRAS* 453 1587 (2015)
- [20] Goumans T.P.M., Wander A., Catlow C.R.A., Brown W.A. *MNRAS* 382 1829 (2007)
- [21] Goumans T.P.M., Catlow C.R.A., Brown W.A. *J.Chem. Phys.* 128 134709  
535 (2008)

- [22] Goumans T.P.M., Kastner J J. *Chem. Phys. A.* 115 10767 (2011)
- [23] Goumans T.P.M. *MNRAS* 413 2615 (2011)
- [24] Andersson S., Goumans T.P.M., Arnaldsson A. *Chem. Phys. Lett.* 513 31-36 (2011)
- 540 [25] Rimola A., Taquet V., Ugliengo P., Balucani N., Ceccarelli C., *A&A* 572 A70 (2014)
- [26] Korchagina K.A., Spiegelman F., Cuny J. J. *Phys. Chem. A* 121 9485-9494 (2017)
- [27] Woon D.E. *Astrophys. J.* 569 541-548 (2002)
- 545 [28] Seng L. Kästner J. *Astrophys. J.* 850 (2017)
- [29] Wakelam V., Loison J-C., Mereau R., Ruaud M. *Mol. Astrophys.* 6 22-35 (2017)
- [30] Cazaux S., Minisalle M., Dulieu F., Hocuk S. *A&A* 585 A55 (2016)
- [31] P. Giannozzi, S. Baroni, N. Bonini, M. Calandra, R. Car, C. Cavazzoni, D. Ceresoli, G. L. Chiarotti, M. Cococcioni, I. Dabo, A. Dal Corso, S. Fabris, G. Fratesi, S. de Gironcoli, R. Gebauer, U. Gerstmann, C. Gougoussis, A. Kokalj, M. Lazzeri, L. Martin-Samos, N. Marzari, F. Mauri, R. Mazzarello, S. Paolini, A. Pasquarello, L. Paulatto, C. Sbraccia, S. Scandolo, G. Sciauzero, A. P. Seitsonen, A. Smogunov, P. Umari, R. M. Wentzcovitch, J.Phys.: Condens. Matter, 21, 395502 (2009)
- 555
- [32] Berland K. and Hyldgaard P., *Phys. Rev. B* 89, 035412 (2014)
- [33] Berland K., Cooper V.R., Lee K., Schröder E., Thonhauser T., Hyldgaard P., Lundqvist B.I. *Rep. Prog. Phys.* 78, 066501 (2015)
- [34] T. Thonhauser, S. Zuluaga, C.A. Arter, K. Berland, E. Schröder, P. Hyldgaard, *Phys. Rev. Lett.* 115, 136402 (2015)
- 560

- [35] Morisset S., Rougeau N., Teillet-Billy D. Chem. Phys. Lett. 679 225-232 (2017)
- [36] Moaied, J.A. Moreno, M.J. Caturla, F. Yndurain, J.J. Palacios, Phys. Rev. B 91 (2015) 155419.
- 565 [37] Zhang Y.H., Chen Y.B., Zhou K.G., Zeng C.H., Zhang H.L., Peng Y. Nanotechnology 20 18 (2009)
- [38] Leenaerts O., Partoens B., Peeters F.M., Phys. Rev. B 125416 (2008)
- [39] Ao Z.M., Yang J., Li S., Jiang Q. Chem. Phys. Lett. 461 276 (2008)
- [40] Wilson J., Faginas-Lago N., Vekeman J., Guesta I.G., Sánchez-Marín J.,  
570 Sánchez de Méras A. ChemPhysChem 19 774 (2018)
- [41] Chi M., Zhao Y-P Computational Materials Science 46 1085-1090 (2009)
- [42] Noble J.A., Theulé P, Mispelaer F., Duvernay F., Danger G., Congiu E.,  
Dulieu F., Chiavassa T., A&A 543 A5 (2012)
- [43] Bolina A.S., Wolf A.J., Brown W.A. J. Chem. Phys. 122 044713 (2005)
- 575 [44] Schröder E. Journal of Nanomaterials vol 2013(Article ID 871706)
- [45] Xu Z.F., Raghunath P., Lin M.C. J. Phys. Chem. A 119 7404-7417 (2015)
- [46] Computational Chemistry Comparison and Benchmark  
DataBase, <https://cccbdb.nist.gov/>
- [47] O.K. Rice, H.C. Ramsperger, J. Am. Chem. Soc. 49 1617 (1927)
- 580 [48] L.S. Kassel, J. Phys. Chem. 32 225 (1928)
- [49] Cernicharo J., Marcelino N., Roueff E., Gerin M., Jiménez-Escobar A.,  
Muñoz Caro G.M. ApJL 759 L43 (2012)
- [50] Bermudez C., Bailleux S., Cernicharo J. A&A 598 A9 (2017)
- [51] Koziol L., Wang Y., Braams B.J., Bowman J.M., Krylov A.I. J. Chem.  
585 Phys. 128 204310 (2008)

